HYDRAULICS OF 3D-AERATOR WITH LATERAL ENLARGEMENTS ON SPILLWAYS

FEI MA
Hohai University, Nanjing, China, mafei921@163.com

JIAN-HUA WU
Hohai University, Nanjing, China, jhwu@hhu.edu.cn

KUNPENG SU
Hohai University, Nanjing, China, kunpengsu@yahoo.com

JIANRONG XU
Powerchina Huadong Engineering Corporation Limited, Hangzhou, China, xu_jr@ecidi.com

ABSTRACT

Aerator is an effective element to entrain air into flow for protecting spillways from cavitation damage. However, many spillway side wall had been damaged due to lack of air entrainment near the side wall surface. As a result, 3D-aerator has been introduced for protecting both of bottom and side surfaces of spillways. The present study investigates the performance of a 3D aerator with lateral enlargement for discharge tunnels on a physical model. Results with respect to water fins height, air concentration distribution and lateral cavity length are presented in the form of non-dimensional plots. From this study, the non-dimensional water fin height increases as the lateral enlargement width, the bottom cavity length, approach Froude number. It is also found that the lateral air entrainment can protect the side walls of discharge tunnel from cavitation damage. Based on theoretical analysis, the lateral cavity length is determined by the approach flow Froude number and the ratio of lateral enlargement width to channel width. The paper also presents an empirical expression of lateral cavity length for the 3D aerator with lateral enlargements.

Keywords: 3D-aerator, lateral enlargements, air concentration, lateral cavity length, water fins

1. INTRODUCTION

High heads and large discharges are available to perennial rivers for hydropower generation in southwest region in China. Many such hydroelectric projects are being constructed, such as Wudongde and Baihetan dams (Jia et al. 2009). Because of narrow river gorges, limited available spillways over dam body, the discharge tunnels become very important for disposal of flood. In the design of large discharge tunnels, it is necessary to prevent the risk of cavitation erosion. A conventional method to prevent cavitation erosion in high-velocity flow is achieved by bottom aerators (Russelalnd & Sheehan, 1974; Chanson, 1989, and Michael & Hager, 2010). The bottom aerators separate the flow from the bottom, and the air can enter into the flow through the lower surface in the cavity zone due to the high turbulence eddies close to the air-water interface. As a quite widespread practice and a successful countermeasure, bottom aerators are applied at almost all release works with high head since 1960 (Russelalnd & Sheehan, 1974; Michael & Hager, 2010; & Bhosekar, Jothiprakash, & Deolalikar, 2012).

Most release works have been protected from cavitation damage thanks to bottom aerators. But the discharge tunnel of Ertan hydropower station in China is a special failure case, because the serious cavitation damage had occurred at the tunnel sidewall. It indicates that, for large release works with high head and large discharge, a large black water zone on side wall downstream of bottom aerator may lead to cavitation damage. The previous studies demonstrate that the 3D aerator may completely eliminate the area which is nearby the un-aerated flow and on the sidewalls beneath the ogee spillway. (Wang, Dai, Yang, Liu, & Yang, 2006). The 3D aerator includes a bottom aerator and two lateral aerators after the working gate or at the free surface flow section of the discharge tunnels.

3D aerator after working gate is widely used due to the need of working gate installation, and so the studies on 3D aerator mainly focus on it in the past (Nie, & Wu, 2002, 2003; Li, Dai, Yang, & Ma, 2011; Zhang, Chen, Xu, Wang, & Li, 2011). With the construction of release works with high head and large discharge, the free surface flow 3D aerator has gained significant interest and popularity among researchers and dam engineers (Liu, & Yang, 2004). The free surface flow 3D aerator includes lateral deflector and lateral enlargements with bottom aerators. Liu et al. suggested that the two kinds of lateral aerator above mentioned can effectively eliminate the black water zone on the side wall of discharge tunnels. Meanwhile, they founded that the small lateral cavity can play an important role for avoiding cavitation damage on the side wall of the tunnel (Liu, Yang, Deng, & Wang, 2006). However, the lateral deflector may cause the intense water fins when the lateral cavity length is larger than the bottom cavity length. Wu et al. presented the characteristics of water fins downstream of 3D aerator with lateral deflectors, based on experimental studies (Wu, Li, Ma, & Qian, 2013).

Very few physical model studies were reported for the hydraulics of 3D aerator with lateral enlargements on discharge tunnels. Thus, a systematic research is needed on the design of lateral enlargements for discharge tunnels. In the paper, the authors will describe a new study of the hydraulic behavior of 3D-aerator with lateral enlargements, including water fin, cavity geometry, and air concentration. Non-dimensional plots are presented for side cavity length and water fin height with respect to Froude number. In addition, the air concentration distribution along the channel downstream of aerator is presented.

2. EXPERIMENTAL SETUP AND METHODOLOGY

Laboratory experiments were carried out in a 31.50 m long, 0.35m wide, and 0.24 m deep rectangular Plexiglass flume at the High-speed Flow Laboratory of Hohai University. The experimental setup consists of a pump, an approach conduit, a large feeding basin, a physical model, and a flow return system. The experimental setup is shown on Fig.1. The 3D aerator is placed at the inclined section of an orifice spillway physical model with the free flow. The water was pumped from a pump to the stilling basin. The feeding basin issues an approach (subscript o) flow of depth h_o and average velocity v_o, resulting in the approach flow Froude number $Fr_o = v_o/(gh_o)^{0.5}$, where g = 9.81 m/s^2, is the gravitational acceleration.

Figure 1. Sketch of 3D aerator with lateral enlargement on orifice spillway

Fig. 2 is the definition sketch of the 3D aerator with lateral enlargements geometry and the flow regime. The geometry parameters of the 3D aerator include: t_r and β are the height and deflect angle of the ramp, t_s is the step height for the bottom aerator; t is the lateral enlargement width, and W = 35 cm and i = 1:4 are the upstream width and bottom slope of the orifice spillway model in the inclined section, respectively. Table 1 is the cases and parameters of the 3D aerator with lateral enlargements. Cases M1 and M2 without bottom aerator are used to compare the hydraulics between 3D aerator and bottom aerator. As shown in Fig.2, the water fins may occur downstream of the 3D aerator. The water bodies exceed the free surface of the flow are called as the water fin in the present work. H_f is the height of the water fins, respectively (Fig. 2 (a)).

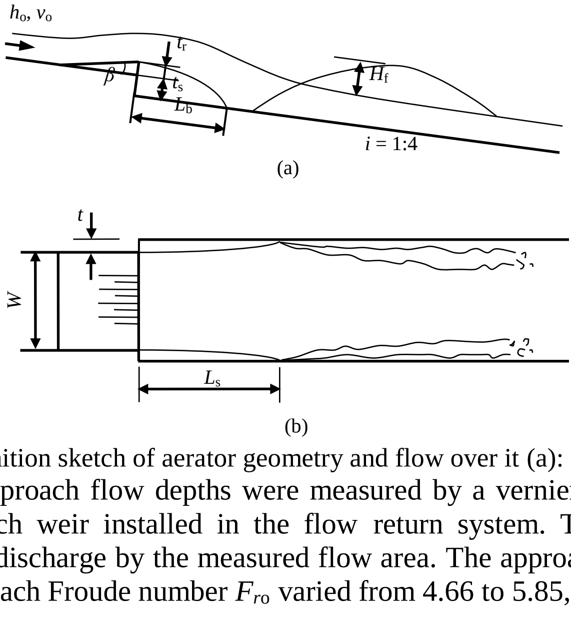

Fig.2 Definition sketch of aerator geometry and flow over it (a): Side view and (b): Plan view

In experiments, the approach flow depths were measured by a vernier depth gage, and the discharges were measured by a V-notch weir installed in the flow return system. The approach flow velocities v_o were measured by dividing discharge by the measured flow area. The approach flow depth h_o varied from 0.076 to 0.160 m, and the approach Froude number F_{ro} varied from 4.66 to 5.85, respectively.

The air concentration (C) gauging points were placed along the channel downstream of the aerator. There were 5 points on the bottom, and 6 points on the side wall. The gauging points of side wall were 3.0 cm from the bottom. The air concentration was recorded using a CQ6-2005 aeration apparatus. The CQ6-2005 aeration apparatus, made by the China Institute of Water Resources and Hydropower Research (Beijing), is a resistance-type of instrument that collects and processes the aeration data on walls by sensors (which contain a pair of parallel electrodes) and a microcomputer. It's sampling rate and period is 1,020 Hz and 10 s, respectively, and the error is 0.3%.

Table 1 Cases and parameters for 3D aerators

Case	t (cm)	t_s(cm)	t_r (cm)
M1	0.5	0	0
M2	1.0	0	0
M3	0.5	3.8	0
M4	1.0	3.8	0
M5	0.5	3.8	1.0
M6	1.0	3.8	1.0

3. RESULTS AND DISCUSSIONS

3.1 Experimental observation

Fig. 3(a) is the flow regime over the lateral enlargements without bottom aerator (case M2). The lateral cavity was formed downstream of the lateral enlargements, and the air was entrained into the flow from the lateral cavity. But the entrained air is less according to experimental observation. In addition, the water fins occurred downstream of the lateral enlargements, and it significantly uplifted the flow profile at the side wall. Fig. 3(b) shows the flow regime over the lateral enlargements with bottom offset aerator (case M4). The bottom and lateral cavities simultaneously appeared, and connected each other. In this case, the air entrainment effect is visibly better than the pure lateral enlargements without bottom aerator. However, it caused the larger water fins. According to previous study, the cause of formation of water fins is that the lateral cavity length is larger than bottom cavity length, and the jet consequently jumps from the bottom to flow surface at the lateral cavity. Comparing with case M4, a ramp is added on the bottom offset. In this case, the bottom cavity length was larger than lateral cavity length. As a result, the water fins nearly disappeared, as shown in Fig. 3(c).

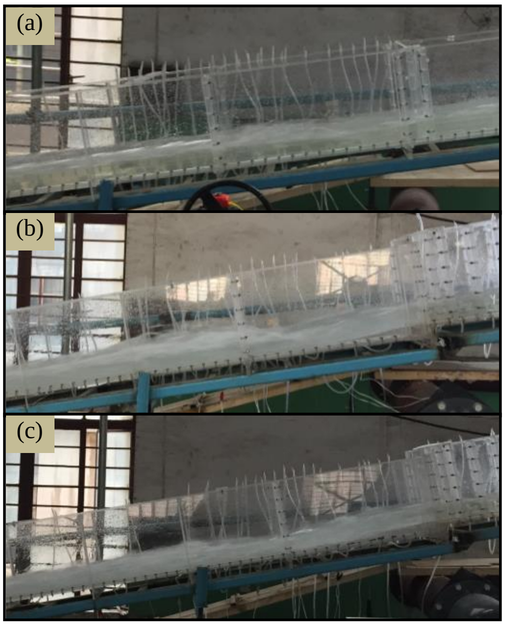

Figure.3 Flow over the aerators (a. M2, b. M4, c. M6; Fr = 5.85)

3.2 Air concentration distribution on side wall

Fig.4 presents the air concentration on the side wall along the flow direction for different cases. Note that the data of gauging points in lateral cavity are not plotted in Fig.4. It can be seen that, for pure lateral enlargements without bottom aerators (M1 and M2), all data of air concentration is nearly less than 2%. Further, the larger lateral enlargement width leads to the larger air concentration for cases M1 and M2. 3D aerators, the lateral enlargements with bottom aerators, obviously promote the effect of air entrainment at the lateral cavity, because the air can be ventilated from the bottom cavity connected with the atmosphere to lateral cavity. As a result, the air concentration data are larger than 1% for cases M3 – M6. However, the larger lateral enlargement width could not remarkably increase the air concentration on side walls. In other word, the smaller lateral cavity may play a good role for protecting the side wall from cavitation damage. Fig.5 is plotted with the air concentration along the side walls under different approach Froude numbers for case M3. At the range of 2 m downstream of the aerator, the air concentration is above 1 -2 % under the different approach conditions. It demonstrates that, for 3D aerator with lateral enlargements, can effectively eliminate the black water zone downstream of the aerator, provides the adequate aerated flow along the side wall.

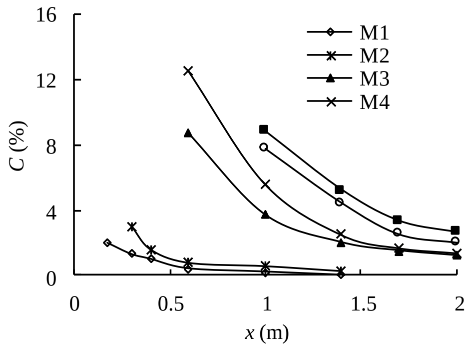

Figure. 4 Air concentration distribution on side walls for different cases（Fr＝4.66）

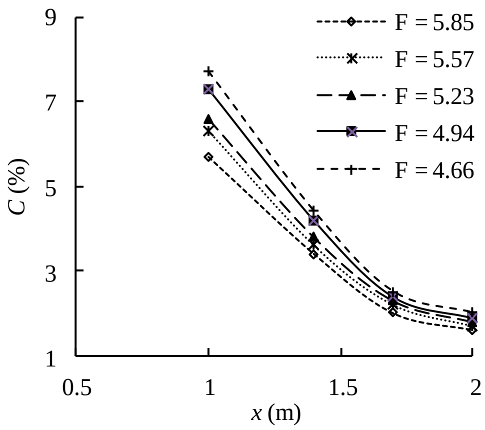

Figure. 5 Air concentration distribution on side walls for different approach Froude numbers（M3）

3.3 Water fins height

The water fins are generated due to the lateral aerators. The water fin height is determined by aerator geometry and approach flow parameters. Fig.6 is the relationships of the non-dimensional water fin height and the approach Froude number for all cases. It indicates that the water fin height increases with the increasing approach Froude number and the enlargement width. For 3D aerator with lateral enlargements, as bottom aerator uses the combination of the offset and the ramp, and the lateral enlargement width is 0.5cm, the water fins will be very slight (the largest water fin height is 0.03cm, M5). In general, the water fins are small for 3D aerators with lateral enlargements. For purpose of control of water fins, the lateral enlargement width should be used under the condition of guarantying enough lateral air entrainment.

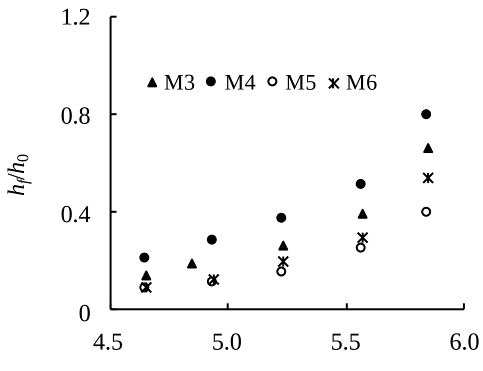

Figure.6 Non-dimensional water fin heights varied with approach Froude numbers

3.4 Lateral cavity length

Fig. 7 presents the non-dimensional lateral cavity lengths varied with the approach Froude numbers for all cases. From the figure, it can be seen that, the lateral cavity length of 3D aerator (M3 – M6) is larger than that of pure lateral enlargements without bottom aerators (M1and M2). It demonstrates the bottom cavity leads to the increase of lateral cavity length. In addition, the larger lateral enlargement width or approach Froude number causes the larger lateral cavity length. In Fig. 7, the difference of lateral cavity lengths of M3 – M6 is small. It indicates that the effect of bottom aerator geometry on the lateral cavity length is slight. So the lateral cavity lengths are the functions of the lateral enlargement width and the hydraulic parameters of the flow, as

$$L_s = f(W, lr, h_o, v_o)$$

Further, Eq.(1) could be rewritten in dimensionless variables as

$$\frac{L_s}{h_o} = f(\frac{lr}{W}, Fr_o)$$

Fig.8 shows the variations of $\frac{L_s}{h_o}$ with $Fr_o(\frac{lr}{W})^{0.15}$. It could be seen that $\frac{L_s}{h_o}$ has good linear relationships with $Fr_o(\frac{lr}{W})^{0.15}$. Based on the data, we have:

$$\frac{L_s}{h_o} = 2.08 Fr_o\ lr^{0.15} - 9.12$$

$$R^2 = 0.915$$

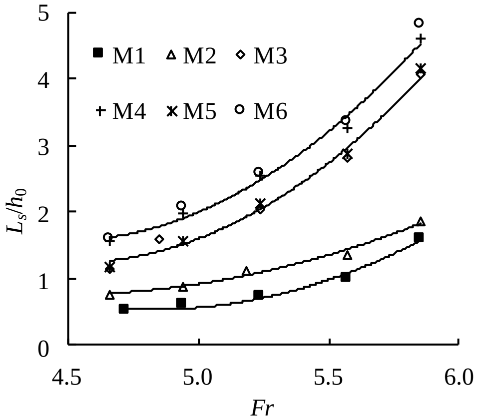

Fig.7 Non-dimensional lateral cavity length virus approach Froude number

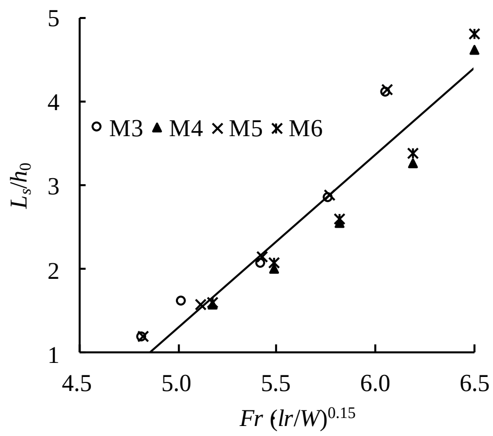

Figure.8 L_s/h_o virus $Fr_o(l_r/W)^{0.1}$

4. CONCLUSIONS

For 3D aerator with lateral enlargements, comparing with pure lateral enlargement without bottom aerator, the lateral cavity length is larger because the bottom cavity provides ventilation vent connected with the atmosphere. The lateral enlargements generate the water fins, while the water fins are slight due to the shorter lateral cavity length related with the bottom cavity length. The results demonstrate that, under the different approach flow conditions, the black water zone downstream of the aerator is eliminated thanks to lateral air entrainment. The lateral cavity length increases with the increasing lateral enlargements width and the approach Froude number. The increase in approach Froude number also causes the increase in non-dimensional water fin height. In additions, the expression of estimating the lateral cavity length is presented in the paper.

REFERENCES

Chanson H. Study of air entrainment and aeration devices. (1989). *Journal of Hydraulic Research*, 27(3): 301-319.

Jia, J.S., Yuan, Y.L., Zheng, C.Y., and Ma, Z.L. (2009). Chinese dam comments in 2008: Statistics, progress and concerns. Available at http://www.chincold.org.cn/chincold/upload/news /lin200911254534542.pdf (in Chinese).

Liu Chao, and Yang Yong-quan. (2004). Study on air entrainment to alleviate cavitations at the end of anti-arc in spillway tunnel. *Journal of Hydrodynamics*, 19(3): 375 - 382 (in Chinese).

Liu Chao, Yang Yong-quan, Deng Jun, and Wang Hai-yun. (2006) Experimental study on air entrainment to alleviate cavitations for downstream sidewalls of ogee-section in spillway tunnel. *Journal of Hydrodynamics*, 21(4): 465 - 472 (in Chinese).

Michael P., and Hager W. H. Chute aerators II: Hydraulic design. (2010). *Journal of Hydraulic Engineering*, 136(6): 360 - 367.

Nie Mengxi, and Wu Guanghao.(2002). Effect of the lateral def lector on cavity design. *Journal of Tsinghua University* (*Science & Technologh*), 42(4): 33 – 37 (in Chinese).

Nie Meng-xi, and Wu Guang-hao. (2003). Effect of lateral deflector on aeration in the bottom and lateral cavities of flows over spillway. *Journal of Tsinghua University*, 43(8): 28 – 36 (in Chinese).

Russelalnd S. Q., and Sheehan G. J.. Effect of Entrained Air on Cavitation Damage (1974). *Canadian Journal of Civil Engineering*, 1: 97-107.

Pinto N. S., and Neidert S. H. Evaluating entrained air flow through aerators. *Water Power Dam Construction*, 1983, 35(8): 40 - 42.

Wang Hai-yun, Dai Guang-qing,Yang Yong-quan, Liu Chao, and Yang Qing. (2006). Characteristic Study on Preventing Cavitation Damage of Hydraulic Structures Side-walls with High Head. *Journal of Sichuan University* (*Engineering Science Edition*), 38(1): 38 - 43 (in Chinese).

Zhang Jian-min, Chen Jian-gang, Xu Wei-lin, Wang Yu-rong, and Li Gui-ji. (2011). Three-dimensional numerical simulation of aerated flows downstream sudden fall aerator expansion in a tunnel. *Journal of Hydrodynamics*, 23(1): 71 - 80.

Wu Jian-hua, Li Dan, Ma Fei, & Qian Shangtuo. (2013). Fin characteristics of aerator devices with lateral deflectors. *Journal of Hydrodynamics*, 25(2): 258 - 263.